Organization of Thin Films of Nanostructured Materials at Air-water and Air-solid Interfaces

Nishtha Agarwal

A dissertation submitted for the partial fulfilment of BS-MS dual degree in Science

Indian Institute of Science Education and Research Mohali
April 2014

Certificate of Examination

This is to certify that the dissertation titled **Organization of Thin Films of Nanostructured Materials at Air-water and Air-solid Interfaces** submitted by **Nishtha Agarwal** (Reg. No. MS09091) for the partial fulfilment of BS-MS dual degree programme of the Institute, has been examined by the thesis committee duly appointed by the Institute. The committee finds the work done by the candidate satisfactory and recommends that the report be accepted.

Dr. Goutam Sheet Dr. Sugumar Venkataramani Dr. Santanu K. Pal

(Supervisor)

Dated: Arpil 25, 2014

Declaration

The work presented in this dissertation has been carried out by me under the guidance of Dr. Santanu K. Pal at the Indian Institute of Science Education and Research Mohali.

This work has not been submitted in part or in full for a degree, a diploma, or a fellowship to any other university or institute. Whenever contributions of others are involved, every effort is made to indicate this clearly, with due acknowledgment of collaborative research and discussions. This thesis is a bonafide record of original work done by me and all sources listed within have been detailed in the bibliography.

Nishtha Agarwal
(Candidate)

Dated: April 25, 2014

In my capacity as the supervisor of the candidates project work, I certify that the above statements by the candidate are true to the best of my knowledge.

Dr. Santanu K. Pal
(Supervisor)

Acknowledgment

I express my deep sense of gratitude and profound feeling of admiration to Dr. Santanu Pal for his advice, expert guidance, valuable suggestions, discussions and constant encouragement during the entire course of this work and preparation of the thesis. I have really enjoyed the work under his guidance.

I am also grateful to my Master thesis committee members Dr. Sugumar and Dr. Goutam Sheet for their valuable suggestions and comments during the committee meetings.

I am highly grateful Dr. Sandeep Kumar, RRI for his valuable suggestions and guidance during my work at RRI and Dr. Goutam Sheet for his guidance during AFM measurements. I would also like to thank Dr. Anant Venkateshan for SEM and STEM.

I owe greatly to Ashima Arora, Monica Gupta and Avinash(RRI) who have helped me greatly in this research work. I would also like to thank my other lab mates for their support and discussions.

I thank all my friends for the and all my batch mates who provided a wonderful and friendly atmosphere to carry out research during the entire period. It is my pleasure to thank each and every member of the Department of Chemical sciences who have helped me in various ways during the course of investigation and research.

I wish to acknowledge Prof. N. Sathyamurthy, Director, IISER Mohali, for allowing me to use the various facilities of this institute to carry out the research work.

I express my sincere gratitude my parents and my brother for their encouragement and moral support throughout the course of study.

I would also like to acknowledge the Department of Science and Technology, India for providing INSPIRE fellowship.

List of Figures

List of Symbols used in the thesis

π	Surface Pressure
π_c	Collapse Pressure
π_t	Target Pressure
A_m	Area per molecule
A_o	Limiting area per molecule
γ_o	Surface Tension of pure water
γ	Surface Tension of water with monolayer

List of Abbreviations used in the thesis

LC	Liquid Crystal
LM	Langmuir monolayer
LB	Langmuir Blodgett
A-W	Air-water
A-S	Air-solid
AFM	Atomic force microscope
BAM	Brewster angle microscope
TRP	triphenylene
H6TP	Hexamethyl triphenylene
TOP	trioctylphosphine
TOPO	trioctylphosphine oxide
TCB	Azobenzene based mesogen
HMDS	hexamethyldisilazane
ESP	Equilibrium spreading pressure
SEM	Scanning Electron Microscope
STEM	Scanning Transmission Microscope
QD	Quantum dots
NP	Nanoparticles

Abstract

This thesis deals with the studies on assembly and organization of amphiphilic molecules at air-water and air-solid interfaces. Molecules consisting of hydrophilic and hydrophobic parts are known as amphiphilic molecules or amphiphiles. These molecules when spread at air-water interface, the hydrophilic part anchors to the water and the hydrophobic part stays away from the water. If there is a proper balance between the hydrophilic and hydrophobic parts, these molecules form insoluble monolayer at air-water interface called Langmuir monolayer.

Langmuir monolayer can be used as a model system to study the properties of two dimensional systems. Langmuir monolayers can be transferred from the air-water interface onto the solid substrates by Langmuir-Blodgett (LB) technique to obtain LB films. These films can be studied using techniques like atomic force microscope (AFM). Different modes of AFM can be used to study the topography, electrical and mechanical properties of the LB films.

The scope of this thesis is as follows:

The first chapter of the thesis gives a brief introduction to liquid crystals (LCs), their different types based on structure and properties. Then it continues with a short introduction to Langmuir monolayers and Langmuir Blodgett thin films.

The second chapter deals with the self-organization of LC mesogen at air-water and air-solid interface. Recently azobenzene based novel mesogen has been synthesised in our laboratory, which has been used to form Langmuir Monolayers and LB thin films. Temperature dependent AFM studies have been carried out.

The third chapter deals with study of CdSe quantum dots - discotic LCs composites at air-water and air-solid interfaces. LC Nanoscience has a lot of potential applications in many devices such as solar cells, biosensors, etc. Thus, our efforts to study thin films of such composites might be useful in such thin film devices.

The fourth and final chapter concludes the work and mentions about the future work that will be carried out.

Contents

Chapter 1

Introduction

1.1 Liquid Crystals

LCs are a state of matter which has properties intermediate to that between liquids and crystals. In liquids, the molecules are mobile and have no orientational or positional order. In crystals, the molecules have no mobility and are located in regular repeating positions. This leads to long range order in both position and orientation [1]. In LCs, the molecules exhibit intermediate properties; a combination of both order and mobility (Figure 1.1). For this reason, they are also called mesophases and the molecules that display such properties are called mesogens. When molecular crystals are heated to their melting point, they usually change directly into the liquid state. The periodic structures of the lattice as well as the orientational ordering of the molecules are destroyed simultaneously. However due to anisotropy in constituent molecules, there is disappearance of orientational order before the melting of the lattice which leads to certain degree of fluidity[3]. The molecules can slide over each other while preserving the parallelism. The fluid is therefore anisotropic and like crystals,

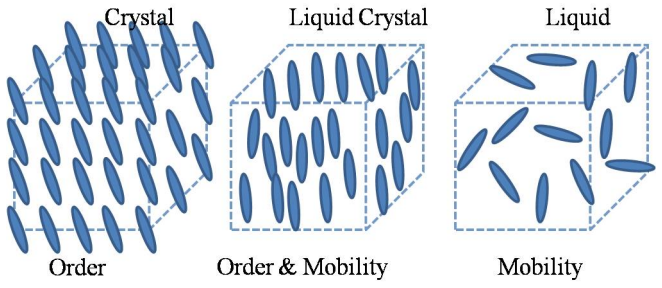

Figure 1.1: Difference between crystal, LC and liquid.

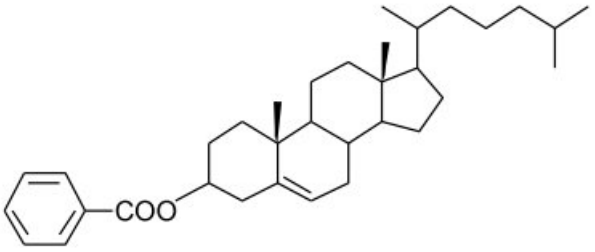

Figure 1.2: Cholesteryl benzoate (1)

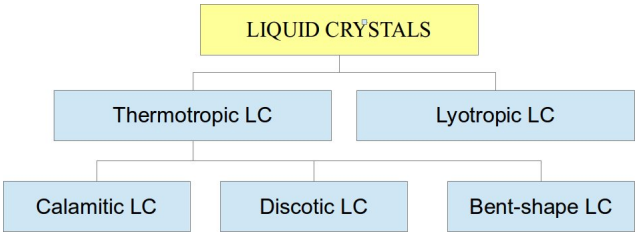

Figure 1.3: Classification of LCs

show optical birefringence and dielectric anisotropy. On increasing the temperature, they transform into isotropic clear liquid. The term was coined by Otto Lehmann who performed polarized optical studies on cholesteryl benzoate [4](Figure 1.2). This molecule was found to be having double melting point by botanist Friedrich Reinitzer [5]. He had synthesised several esters of cholesterol. He observed that crystal of this material melted at $145.5\,\mathrm{deg}\,C$ into a cloudy fluid, which upon further heating to $178.5\,\mathrm{deg}\,C$ became clear.

1.1.1 Classification of LCs

LCs are generally classified into two broad areas:

1 Thermotropic, whose mesophase formation is temperature dependent

2 Lyotropic, whose mesophase formation is solvent and concentration dependent.

The classification is is shown in Figure 1.3. We have mainly worked with thermotropic LCs for thin film studies. The thermotropic LCs are of interest from the standpoint of both basic research as well as applications in electro-optic displays, temperature and pressure sensors.

In the following section, thermotropic LCs have been described and their classification has been explained.

1.1.2 Thermotropic LCs

The term thermotropic arises because transitions involving these mesophases are effected by change in temperature. The essential requirement to be a thermotropic LC is a structure consisting of a central core (often aromatic) and a flexible peripheral moiety (generally aliphatic chains). Based on the shape of the mesogenic molecules, thermotropic LCs have been classified into three main structural groups (Figure 1.3).

Calamitic LC

Rod like molecules with rigid core and flexible chains can exhibit LC phases. Such LCs are known as calamitic LCs. Common phases exhibited by these materials are explained below.

1 Nematic Phase
In nematic LC phase, the molecules have only long range orientational order and no positional order. This is the least ordered LC phase. The word nematic comes from the Greek word *nematos* meaning thread. It refers to certain thread like defect patterns observed in this phase under the polarizing microscope. Calamitic molecules when cooled from isotropic phase can form nematic phase by spontaneous orientation of their long axis approximately parallel to a preferred direction. The preferred direction is called the director and is represented by an apolar unit vector **n**. Figure 1.4 shows the schematic representation of nematic phase exhibited by calamitic molecules.

2 Cholesteric Phase
Cholesteric phase which is also known as chiral nematic phase is exhibited by such mesogenic molecules which are chiral[1] in nature or have chirality induced in them by doping nematic LCs by chiral molecules. In this phase all the molecules on an average arrange parallel to the director **n** just like in the nematic phase. However, the asymmetry in the constituent molecules causes a slight and gradual spontaneous rotation of the director as shown in schematic (Figure 1.5). The

[1] An object or molecule is said to be chiral if it does not superimpose onto its mirror image

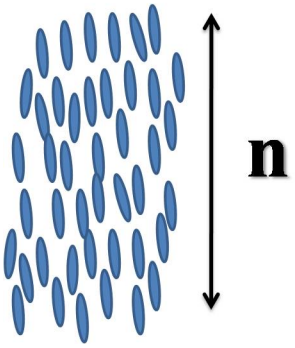

Figure 1.4: Schematic representation of nematic phase.

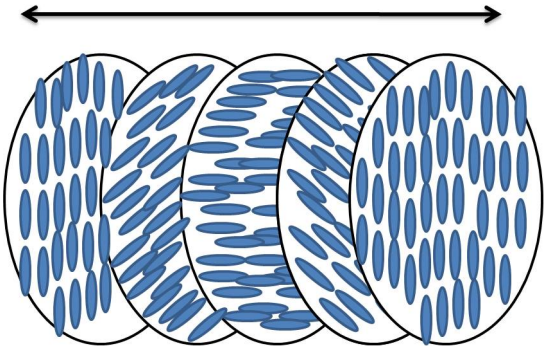

Figure 1.5: Schematic representation of Cholesteric phase. Arrow shows half a pitch.

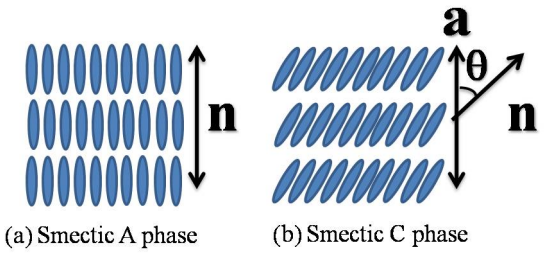

Figure 1.6: Schematic representation of Smectic A and Smectic C phase.

director describes a helix with a specific temperature dependent pitch.

3 Smectic Phase
In smectic LCs, the molecular organization has translational order in one dimension and liquid-like positional order in other directions. Smectic LCs are layered structures with specific interlayer spacing. Within a layer the molecules possess liquid like order. The long molecular axis on an average is oriented collectively along one direction (**n**).If **n** is parallel to layer normal then the smectic phase is known as Smectic A phase and if **n** makes an angle (θ) with the layer normal a it is known as Smectic C phase (Figure 1.6).

Discotic LC

Molecules with flat, rigid, disc shaped core and flexible parts at the periphery can exhibit LC phases called discotic LCs. The self-organization of the molecules due to interaction between the discotic cores, leads to the formation of various LC phases [7]. They mainly consists of flat aromatic ring to which flexible alkyl chains can be attached. Various aromatic cores with different molecular architectures have been reported to exhibit discotic phase. Examples of cores used to synthesize the discotic LCs are benzene, triphenylene, anthraquinone, hexabenzocoronene,phthalocyanine, decacyclene etc.

The discotic molecules can self-organize due to strong $\pi - \pi$ interaction between the aromatic cores and form column like structures. The length of the flexible peripheral substituents will determine the intercolumnar distances. These strong interactions between the cores results in the high charge mobility along the column axis as compared to the charge mobility in the direction perpendicular to the column axis. This high anisotropy in the charge mobility results in quasi-one dimensional conductivity

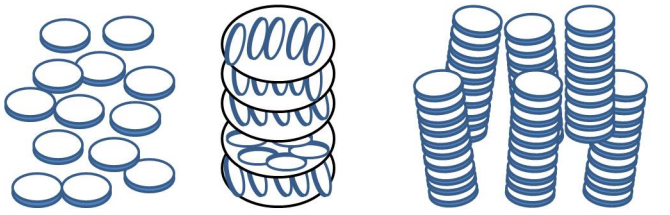

Figure 1.7: Schematic representation of discotic nematic phases exhibited by disc shaped molecules. (a) Shows nematic phase (b) shows chiral discotic nematic phase and (c) shows nematic columnar phase.

behavior. Because of this, DLC find applications in devices like field effect transistor, light emitting diode and photovoltaic solar cell. Hence these materials constitute as a new generation of organic semiconductors [8].

Like calamitic molecules, the discotic molecules also exhibit various LC phases depending on the organization of molecules. These LC phases can be broadly classified into following two categories:

1 Discotic Nematic phase
This phase is similar to the nematic phase exhibited by calamitic LCs. In this phase the molecules have only long range orientational order but no positional order. The molecules more or less stay parallel to each other and have full translational and rotational freedom about their short axis. Their long axes which span the plane of discotic core orient parallel to a general plane. If the discotic molecules are chiral in nature or if chiral dopant is added into discotic LCs, the material may exhibit chiral discotic nematic phase (Figure 1.7).
Also, in some discotic LCs, the molecules may self organize into column like structures. Such a phase is called nematic columnar phase. In this phase, the columns themselves do not have any long range positional order, but have long range orientational order (Figure 1.7).

2 Discotic Columnar phase
In discotic columnar phase, the molecules stack themselves to form column like structures, which organize in a two dimensional lattice. The molecules in each column do not have long range positional order. Depending on the lattice formed by the columns the columnar phase can be classified into various categories viz.,

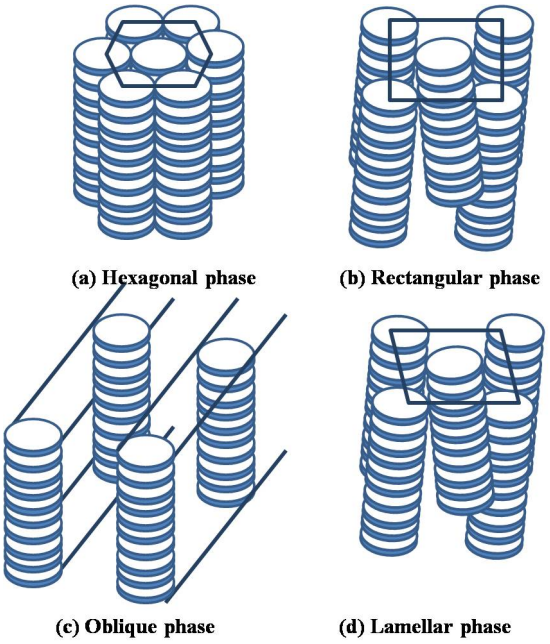

Figure 1.8: Schematic representation of various discotic columnar phases exhibited by discotic molecules. (a) Shows hexagonal phase, (b) shows rectangular phase, (c) shows oblique phase and (d) shows lamellar phase.

hexagonal, rectangular, oblique and lamellar phases as shown in the schematic representation in Figure 1.8.

For Langmuir Monolayers, the important characterstic of a molecule is amphiphilicity.

1.2 Amphiphiles

Molecules containing hydrophilic (water loving) part and hydrophobic (water hating) part are known as **amphiphiles** [9]. Typical examples for amphiphilic molecules are long chain fatty acids like stearic acid ($C_{17}H_{35}COOH$). The carboxyl (-COOH) group of the fatty acids acts like hydrophilic part and the alkyl chain acts like hydrophobic part. Other class of organic molecules containing a hydrophilic group like $-CH_2OH$, $-CN$, $-COO-$, $-CONH_2$, $-CH=NOH$, $-C_6H_4OH$, $-CH_2COCH_3$, $-NHCOCH_3$, etc., along with a balancing hydrophobic group can also be amphiphilic.

When amphiphilic molecules are put on the water surface, the hydrophilic part anchors to the water surface due to its interaction with the water molecules. The hydrophobic

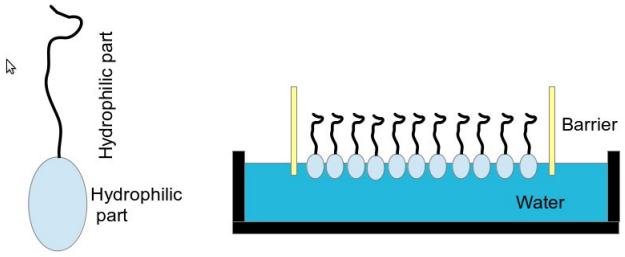

Figure 1.9: Schematic representation of amphiphilic molecules spread over the water subphase to form a monolayer

part of the molecules stay away from the water. If the molecules possess a proper balance of hydrophilic part and hydrophobic part, they spread over the water surface to form a stable monolayer. A schematic is shown in the Figure 1.9 Such mono-molecular films are known as Langmuir monolayers. Since LCs have long alkyl chains, they can comprise of both hydrophilic and hydrophobic part. Hence they can be employed very easily to form langmuir monolayers.

1.3 Langmuir Monolayers

Langmuir monoloayers can be prepared by dissolving amphiphiles in a volatile solvent and spreading the dilute solution over the water surface drop by drop [10]. The volatile solvent evaporates and the molecules spread spontaneously over water surface with hydrophilic group in contact with water and hydrophobic group staying away from the water. There are many thermodynamic parameters like surface density of molecules, temperature etc. A parameter used for study of Langmuir Monolayers is the surface pressure π. It is basically the difference in surface pressure of water with and without monolayer. On compressing the monolayer, there is a decrease in area per molecule(A_m). The phase transitions can be studied as a variation of π as a function of A_m at constant temperature which is called surface pressure-area isotherm or simply isotherm. This is surface manometry[10].

1.3.1 Film Characterization

Surface Manometry

Surface pressure and pressure measurements There is an imbalance of forces at the air/water interface and which leads to presence of surface free energy. Polar liquids,

such as water, have strong intermolecular interactions and thus high surface tension. Any factor such as temperature or any contamination like surfactants, which decreases the strength of this interaction lowers the surface tension [11].
This interfacial free energy is accessible by measurements of the surface tension, γ. The surface tension of water is around $73\,mN/m$ at $20\,\mathrm{deg}\,C$ which is an exceptionally high value that makes it an excellent subphase [12].
On addition, the solution spreads rapidly to cover the available area. As the solvent evaporates, a monolayer is formed. When the available area for the monolayer is large the distance between adjacent molecules is large and their interactions are weak. The monolayer can then be regarded as a two-dimensional gas[11,12]. Under these conditions the monolayer has little effect on the surface tension of water. If the available surface area of the monolayer is reduced by the barrier system the molecules start to exert a repulsive effect on each other. This two-dimensional analogue of a pressure is called surface pressure and is measured by Wilhelmy plate method. Measurement is made by determining the force due to surface tension on a plate suspended so that it's partially immersed in the subphase [11,12].

Brewster Angle Microscopy

Brewster angle microscope commonly known as BAM, can be used to visualize the phases exhibited by the monolayer at air-water interface. When a light is incident on an interface at an angle equal to Brewster angle, the reflected light will have almost zero in-plane polarization (p-polarization) component. This phenomenon can be found when the light is reflected by a denser medium [13].
In our experimental setup, the p-polarized laser beam of wavelength 586 nm is incident on the water surface at Brewster's angle (53.1 deg). Hence, the reflection from the pure water surface will be zero. In the presence of the monolayer, the refractive index of the interface changes and the Brewster angle condition is no more satisfied. This results in the non-zero p-polarized component in the reflected light. This gives the contrast. The reflectivity at the interface is dependent on the factors like thickness, roughness and anisotropy of the monolayer. Domains with different orientation or tilt of the molecules will give rise to different contrasts, thus helping us to visualize the different phases exhibited by the monolayer [14].

1.4 Langmuir Blodgett Films

Langmuir monolayers can be transferred onto a solid substrate using the Langmuir-Blodgett (LB) technique [15]. Such thin organic films of a thickness of a few nanometres are the source of high expectations as being useful components in many practical and commercial applications such as sensors, detectors, displays and electronic circuit components [11,12, 16]. There are many techniques for thin film deposition such as thermal evaporation, sputtering, and electrodeposition, and molecular beam epitaxy, adsorption from solution, self assembly and Langmuir-blodgett film deposition. The LB deposition technique is perhaps the most promising of such techniques because it allows the fabrication of ultra-thin, highly ordered films [11]. In the LB method, Langmuir monolayer is transferred onto a solid substrate, and this process can be repeated with the same substrate to form multilayer films of same or different composition.

The LB-technique is one of the most promising techniques for preparing such thin films as it enables

1 The precise control of the monolayer thickness.

2 Homogeneous deposition of the monolayer over large areas.

3 The possibility to make multilayer structures with varying layer composition.

An additional advantage of the LB technique is that monolayers can be deposited on almost any kind of solid substrate

1.4.1 Film Fabrication

The equipment used for deposition of films is referred to as Langmuir trough (Figure 1.10). The apparatus present in our lab is Langmuir-Blodgett film deposition system by Apex Instruments LB2007DC. It consists of Teflon trough which holds the liquid subphase on which the monolayer is spread; and two Delrin square bars to enable film compression. And other measuring apparatus for film characterization which includes position detectors to measure the surface area of the film and surface pressure sensor (Figure 1.10).

Highly organized multilayer can be accomplished by successively dipping a solid substrate up and down through the monolayer while keeping the surface pressure constant. A good deposition will depend not only on the nature of the monolayer molecules themselves, but also on subphase conditions such as pH, temperature, and

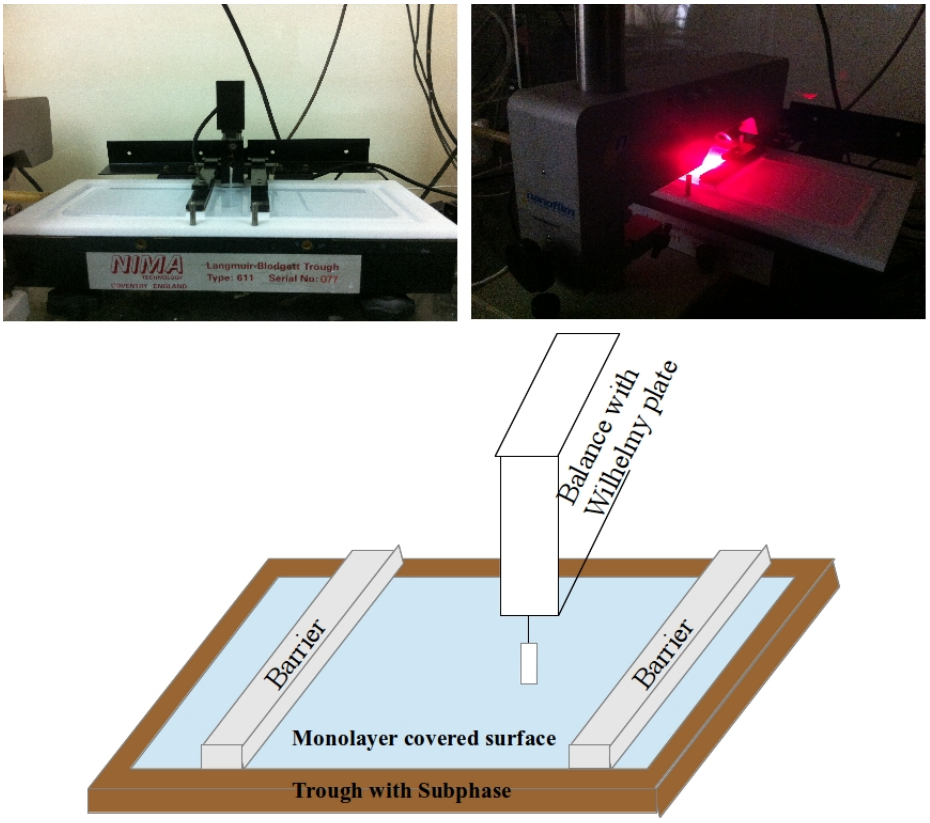

Figure 1.10: Langmuir-blodgett thin film deposition film

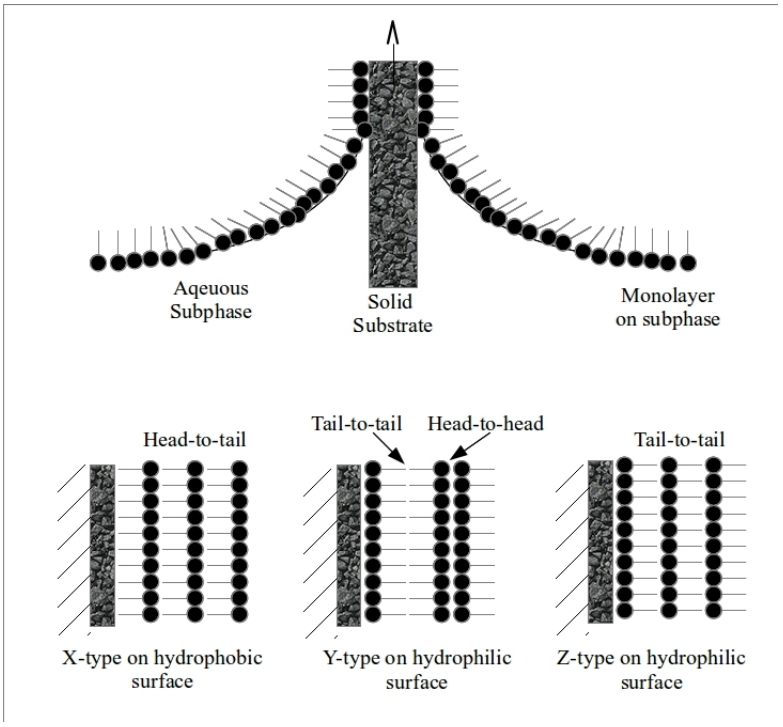

Figure 1.11: Deposition of Langmuir-blodgett film

ionic contents, on the speed of immersion and withdrawal of the substrate (dipping speed) and on whether the substrate is hydrophilic or hydrophobic [16].
There can be either head-to-tail type deposition which generally takes place on hydrophobic substrate, or it can be tail-to-tail/head-to-head or tail-to-head and it takes place on hydrophilic substrate (Figure 1.11).

1.4.2 film Characterization

Atomic Force Microscopy

Atomic force microscopy can be used to get the surface morphology and topography information with very high resolution. In AFM, the force between the tip and the sample is measured as a function of position. AFM is a scanning probe microscopy technique which can be used for all kinds of surfaces irrespective of their mechanical, optical and electrical properties. We use Asylum Research MFP 3D for all our afm studies.

AFM cantilevers and tips are usually made up of silicon or silicon nitride as it is easy to microfabricate these materials using established techniques. The radius of the tip on the cantilever is usually a few nanometers or a few tens of nanometers. The

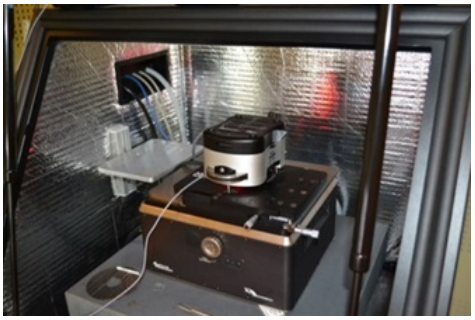

Figure 1.12: Asylum Research MFP 3D system.

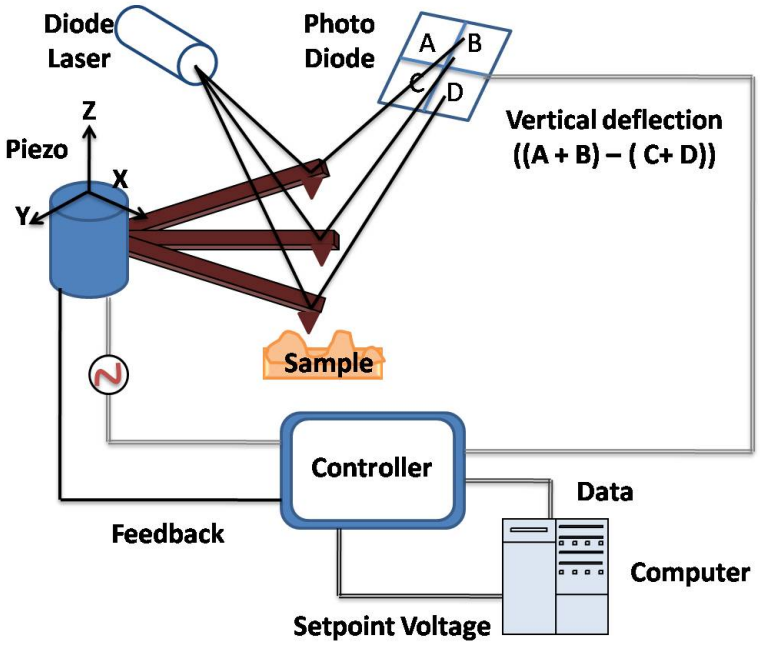

Figure 1.13: Schematic diagram of non-contact mode AFM.

force between the tip and the sample is calculated from the deflection of cantilever that occurs due to the tip-sample interaction. It can be operated in Contact Mode or Non-contact mode.There is also an intermittent contact or tapping mode AFM.

Non-contact mode

In non-contact mode AFM, attractive forces which are of long range are used to monitor the tip-sample interaction. In the non-contact mode AFM, the cantilever is deliberately excited by an electrical oscillator (Figure 1.12).

As the cantilever approaches the sample surface, the tip-sample interaction reduces the amplitude of cantilever oscillation. The sample surface is scanned at constant

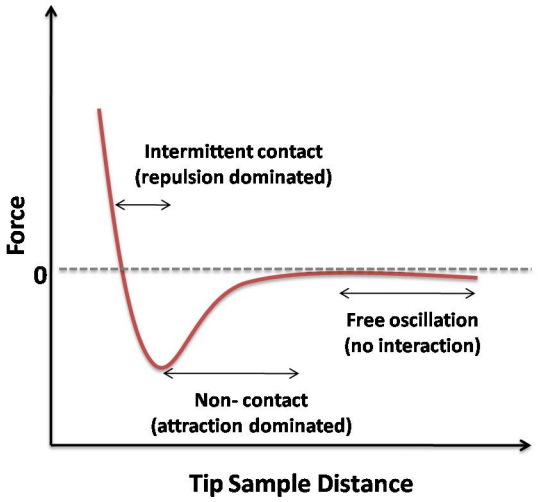

Figure 1.14: Schematic diagram of non-contact mode AFM.

amplitude using a feedback. The change in Z-position of the cantilever gives the topography information (Figure 1.13).

We have also used stage heater to scan the surface morphology at different temperatures.

Bibliography

[1] P. G. de Gennes, and J. Prost, *The Physics of Liquid Crystals*, Oxford University Press: UK, Second edition **2001**.

[2] Nayak, A. Organization of Discotic Mesogenic Amphiphiles at Air-Water and Air-Solid Interfaces, Jawaharlal Nehru University, **2008**.

[3] P. J. Collings, and M. Hird, *Introduction to Liquid Crystals: Chemistry and Physics*, Taylor and Francis: London, **1997**.

[4] O. Lehmann, *Z. Phys. Chem.* **1889** 8, 462.

[5] F. Reinitzer, *Monatsh Chem.*, **1988** 9, 421; for English translation see *Liq. Cryst.* **1989** 5, 7.

[6] Kumar, B. Assembly and Organization of Structurally Novel Amphiphilic Molecules at Air-Water and Air-Solid Interfaces, Jawaharlal Nehru University, **2009**

DLC

[7] S. Chandrasekhar, B. K. Sadashiva, and K. A. Suresh, *Pramana* **1977** 9, 471.

[8] D. Demus, J. Goodby, G. W. Gray, H. W. Spiess, V. Vill *Handbook of Liquid Crystals*, Wiley-VCH, Weinheim **1998**.

[9] G. L. Gaines Jr., *Insoluble Monolayers at Liquid Gas Interface*, Interscience: New York, **1966**.

[10] V. M. Kaganer, H. Mohwald, and P. Dutta, *Rev. Mod. Phys.* **1999** 71, 779.

[11] Zasadzinski, J. A. Viswanathan, R., Madsen, L., Garnaes, J., Schwartz D. K., *Science*, **1994**, 263, 1726-1733.

[12] Roberts, G., Ed. *Langmuir-Blodgett Films*, Plenum Press, New York, **1990**.

[13] G. A. Overbeck, D. Honig, and D. Mobius, *Langmuir* **1993** 9, 555.

[14] E. Teer, C. M. Knobler, S. Siegel, D. Vollhardt, and G. Brezesinski, *J. Phys. Chem. B* **2000** 104, 10053.

[15] Oliveira, O. N., Brazilian Journal of Physics, **1992**, 22, 60.

[16] K. B. Blodgett, *J. Am. Chem. Soc.* **1935** 57, 1007.

Chapter 2

Self-organization of Novel Azobenzene Based Nematic LCs at Air-water and Air-solid Interfaces

2.1 Introduction

Molecular ordering and structuring is often different in thin films than bulk [1]. In recent years, much attention has been paid towards films of organized assemblies such as Langmuir-Blodgett films owing to the intrinsic control of the internal layer structure down to a molecular level (monolayer) and the precise control of the resulting film thickness [2,3]. Study of such monolayer films at air-water interfaces are of great interest because it helps us to understand the packing of molecules based on their structure, different intermolecular interactions etc. which are as such absent in the bulk [4]. Stable films can be transferred onto various substrates which can be easily controlled by the hydrophilicity or hydrophobicity of the solid support. This offer routes to tune the layer architecture according to the demands of the desired molecularly engineered organic thin-film devices. In this paper, we report synthesis of a new series of mesogenic azobenzene based materials and their self-organization at air-water and air-solid interfaces. In contrast to previous studies, the azobenzene-based mesogens reported in this paper show the reversible formation of aligned fibres in the mesophase, making them suitable for devices involving photomechanics, optical switching and others.

Photoactive molecules with different molecular architectures have been used for thin film devices. Among them, azobenzene is the most widely studied photoactive molecule

and holds a special place in molecular devices because of its photosensitivity. For example, utilizing the optical alignment of the azobenzene groups, anisotropic gels [5] and copolymers [6] have been prepared that can be used for a number of potential applications. Azobenzene-containing amphiphilic complexes containing complementary hydrogen bond pairs were shown to form thermally stable bilayer membrane with varied chromophore orientations [7]. The photochroism of azobenzene has been used for the photomodulation of DNA-based molecules in research into the regulation of various bio-reactions [8,9]. In addition, azobenzene serves as a unique core for LCs (LCs) as a photo-responsive trigger. The trans- form of azobenzene derivatives stabilizes a LC phase when dispersed in a LC host because of their rod-like molecular shape which is similar to that of the host LC molecule whereas the cis- isomer shows a bent shape and destabilizes the LC phase [10-13] The self-organization ability of LC material and the photo-orientation ability of the azo- group influence each other mutually [14] which means that the change in molecular alignment is amplified by the cooperative motion. LC phase becomes light sensitive (when azobenzene incorporated into LC systems) on photo-isomerization of the azobenzene moiety. Although it makes difficulty in measuring the clearing temperatures of the azobenzene-containing LC, it provides a new opportunity for switching controlling the anisotropic properties of the ordered phase [15].

A numerous examples are reported on the photo-responsive nature of the azobenzene moiety in thin films [16]. Photo-isomerization can bring in-situ changes in the molecular structure of the azobenzene chromophore [17] which makes it ideal for many photo-devices such as information storage device [18], molecular switching devices [19], sensors [20], etc. Photo-isomerization kinetics at the air-water interface of the Langmuir monolayer of mesogenic azobenzene dimers have been studied in detail by Suresh et al. [21] Thin films of LC mesogens containing azobenzene group form promising candidates for fabrication of devices as LCs can offer high sensitivity and high control over architecture using LB technique [21,22]. Ozaki and his co-workers have reported phase transitions in LB films of azobenzene-containing long chain fatty acids based on spectroscopic studies on H-aggregates [23,24].

In this chapter, we have synthesized new oligomeric mesogens consisting of an azobenzene-based core attached to which are four 4-cyanobiphenyl units via flexible alkyl spacers (Figure 2.1). The molecules were synthesised in our laboratory of our institute by Monika Gupta (PhD scholar with Dr. Santanu K. Pal). It represents a simple but useful advance in the design of a molecular system that enables fundamental insights

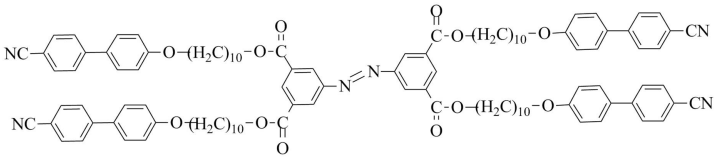

Figure 2.1: Azobenzene based mesogen TCB-10

into unconventional structure-mesophase morphology relationship. Monolayer properties of one of the mesogenic oligomer were studied at air-water and air-solid interfaces. The thin film at the air-water interface was studied using the techniques of surface manometry and Brewster angle microscopy (BAM). The film was transferred onto hydrophilic and hydrophobic solid substrates by vertical LB technique and the wetting behavior was studied using atomic force microscopy (AFM). Our analysis shows that the film transferred onto a hydrophobic silicon substrate dewets to yield nanodroplets associated with mechanism of spinodal dewetting. Temperature dependent AFM topography indicated that the film showed the reversible formation of aligned fibres in the mesophase. Identification of the temperature dependent structural morphology leading to the formation of aligned microstructure is not only fundamentally significant, but also practically important because it enables rational design and controlling the anisotropic properties of the ordered phase for various applications.

2.2 Experiment

Materials and Reagents. Chemicals and solvents were all of AR quality and were used without further purification. Chloroform used for thin film studies was of HPLC grade. The compounds were purified by column chromatography and recrystallization and characterized by Proton Nuclear Magnetic Resonance (^1HNMR), Carbon-13 Nuclear Magnetic Resonance ($^{13}CNMR$), Infra-red (IR), Ultraviolet-visible (UV), Raman spectroscopy and elemental analysis which indicated high purity of the materials. The thermotropic liquid crystalline properties of these materials were investigated by polarizing optical microscopy, differential scanning calorimetry and small angle X-ray diffraction (XRD). Films of TCB-10 were studied using surface manometry, BAM and AFM.

Surface Manometry

The surface manometry experiments were carried out using an APEX LB-2007 and a NIMA 611M trough. The subphase used was ultrapure deionized water obtained from Millipore Milli-Q system. The stock solution of 0.591 mM concentration was prepared using chloroform (HPLC grade, Merck). After spreading it on the air-water interface, the film was left for 20 min, allowing the solvent to evaporate. The $\pi - A_m$ isotherms were obtained by symmetric compression of the barriers with a constant compression rate of $10\,cm^2/min$. The surface pressure (π) was measured using the standard Wilhelmy plate technique. Film stability was also measured in two ways. First, variation of surface pressure (π) was measured with time keeping the area between the barriers constant. Secondly, the change in the area per molecule is measured with time for keeping the surface pressure constant. This enables us to monitor the stability of the film during deposition.

Brewster Angle Microscopy

A Brewster angle microscope (BAM), MiniBAM (NFT, Nanotech,Germany) was employed to observe the films at the A-W interface. Instead of pressure sensor, microscope was put. Images were observed and captured during compression and expansion of the barriers.

Film Deposition

LB technique was employed to transfer various layers of the films onto hydrophilic and hydrophobic substrates at target surface pressure (π_t) with a dipping speed of 1 mm/min. We have employed vertical transfer technique. For hydrophilic surfaces, freshly cleaved mica was used. To obtain hydrophobic surfaces, freshly etched silicon wafers were dipped in hexamethyldisilazane (HMDS) for 12 h and then rinsed with HPLC grade chloroform. Silicon wafers were etched by treating polished silicon wafers for about 5 mins in hot acidic piranha solution (3:1 ratio) which were then rinsed in ultrapure deionized water and then dried.

Atomic Force Microscopy

The atomic force microscope(AFM) studies on these LB films were performed using Asylum Research MFP 3D.We used silicon tips (radius: $92\,nm$) with spring constant

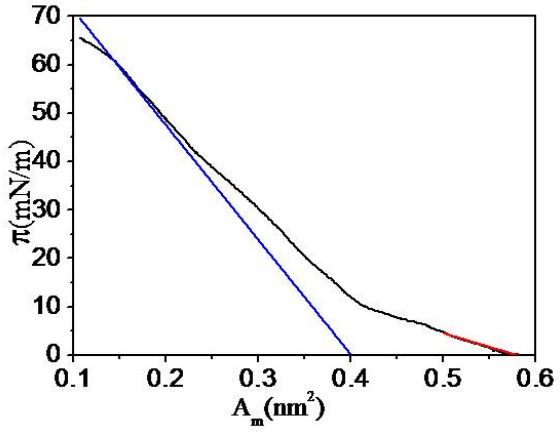

Figure 2.2: Surface pressure (π) - area per molecule (A_m) isotherms of azobenzene-based mesogens synthesized in the study.

of 42 N/m and resonance frequency 300 kHz. Non-contact mode was used to obtain the topography of the film. All the images are shown without any processing.

Surface manometry, BAM and depositions were carried out at room temperature ($25 \pm 0.5 \deg C$). AFM was carried out at different temperatures.

2.3 Results and Discussion

Because of the presence of strong polar groups (such as cyano) and long alkyl chain these molecules are expected to show the monolayer properties (amphiphilic character).We have chosen TCB-10 which showed a monotropic nematic phase on cooling ($114 \deg C$) from isotropic phase ($125.9 \deg C$).
Figure 2.2 shows the surface pressure ($\pi, mN/m$) - area per molecule (A_m, nm^2) isotherm for the compound. At large area per molecule ($A_m > 0.4\, nm^2$) the isotherm shows zero surface pressure. At A_m of around $0.4\, nm^2$ the surface pressure starts increasing upon compression. The film collapses at an A_m of $0.15\, nm^2$ with a collapse pressure of $60\, mN/m$. The high collapse pressure can be attributed to the presence of strong polar groups and strong chain-chain interactions associated with the 4-cyanobiphenyl units via flexible alkyl spacers.

The limiting area per molecule (A_o) value for the expanded phase was found to be $0.57\, nm^2$ while that for condensed phase obtained by extrapolation to zero surface pressure was $0.4\, nm^2$.

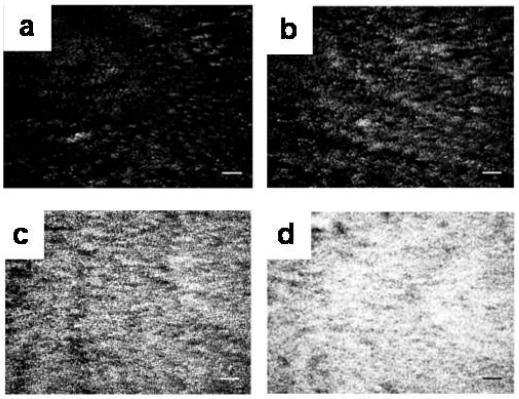

Figure 2.3: The Brewster Angle Microscopy images of compression for TCB-10 at air-water interface. The area per molecule in each case is (a) $0.6\,nm^2$ (expanded phase) (b) $0.5\,nm^2$ (LiquidPhase) (c) $0.4\ nm^2$ (condensed phase) (d) $0.1\ nm^2$ (collapsed state). The scale bar in each image represents 500 μm.

The A_o value remains nearly same for twice the volume spread in the sub-phase. The limiting area corresponds to the edge to edge conformation since the area of the central azobenzene core was calculated to be $0.36\,nm^2$ according to the standard bond length and angles. After collapse, there was a gradual increase in the surface pressure. The BAM images for compression shows that the molecules uniformly come together and form a thin layer. Initially, images show dark region co-existing with grey spots for $A_m > 0.4\,nm^2$. This is 2D gaseous and liquid phase where molecules are relatively far away from each other. On further compression, when $A_m < 0.4\,nm^2$, there is uniform grey region which shows the formation of the monolayer. But on further compression, when the area per molecule is very less,there occurs a collapse for A_m of about $0.15\,nm^2$, where BAM image (Figure 2.3) shows bright regions growing from the grey background. BAM images taken during expansion shows the fibre like pattern formation and the isotherm corresponding to expansion shows high hysteresis (Figure 2.4). This may be due to the supramolecular interactions, in particular, dipolar interactions and $\pi - \pi$ interactions associated with the cyanobiphenyl units. Prominent hysteresis observed in the compression-expansion isotherms confirms the different BAM images (Figure 2.5). Since the molecules are associated and while expansion they form cavities in the middle, there is a rapid decrease in the surface pressure. Since the molecules are associated through non-covalent interactions, they form cavities in the middle during expansion and thus there is a rapid decrease in the surface pressure. The stability of the film was checked by measuring the equilibrium surface pressure at a constant area (Figure 2.6). Further, before deposition, the

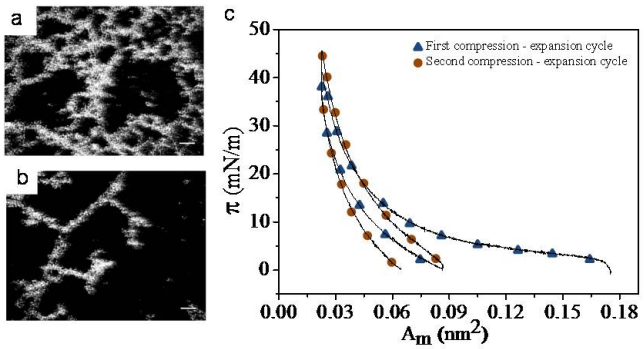

Figure 2.4: The Brewster Angle Microscopy (BAM) images for expansion of TCB-10 at air-waterinterface. The area per molecule is (a) 0.6 nm^2 and (b) 0.8 nm^2.The scale bar in each image represents 500 μm. The plot (c) shows prominent hysteresis for compression-expansion $\pi - A_m$ cycles

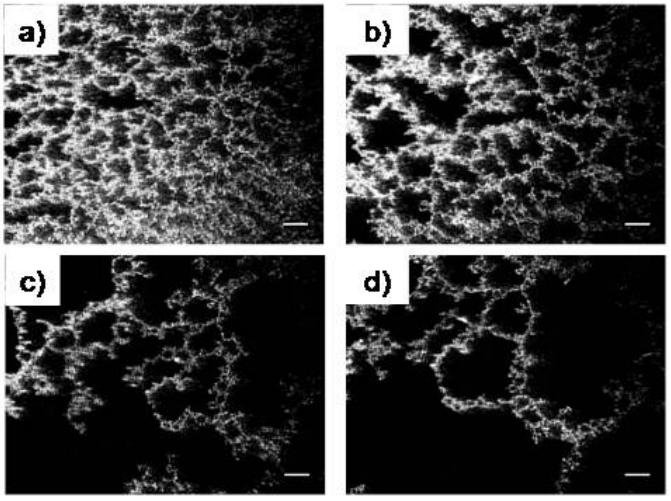

Figure 2.5: BAM images for expansion of TCB-10 at air-waterinterface. The area per molecule is (a) 0.4 nm^2, (b) 0.5 nm^2, (c) 0.6 nm^2 and (d) 0.7 nm^2.The scale bar in each image represents 500 μm.

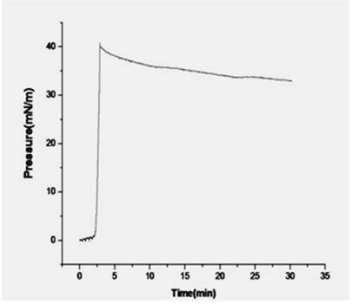

Figure 2.6: Equilibrium Surface Measurement at the surface pressure of 40 mN/m

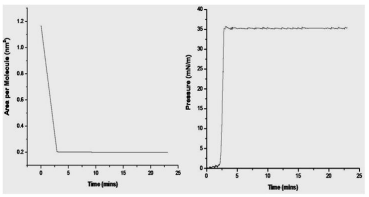

Figure 2.7: Measurement of the stability of the film

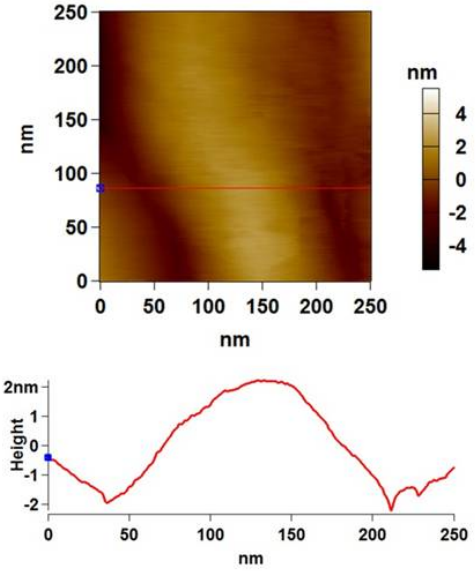

Figure 2.8: AFM topography for film of compound transferred by LB technique onto hydrophilic mica substrate at target surface pressure (π_t) of 35 mN/m showing monolayer region with height profile of about 2 nm. The respective height profile corresponding to the line drawn on the image is shown below.

target pressure of 35 mN/m was achieved and the change in area per molecules was observed to keep the pressure constant (Figure 2.7). By both these measurements we found that film was stable to carry out deposition. Then the film was deposited on hydrophilic mica by vertical dipping. In one dipping cycle, only one deposition takes place in upstroke. The resultant films were characterized by AFM.

The film was transferred onto a hydrophilic mica substrate and studied using AFM. Topography image of the LB film transferred onto a mica substrate at a surface pressure of 35 mN/m is shown in Figure 2.8.

In less dense areas the topography showed a uniform film with a height of about 2.1 nm. This value corresponds to the estimated height of the molecules when four cyano groups are in contact with the water subphase and the alkyl chains together with the

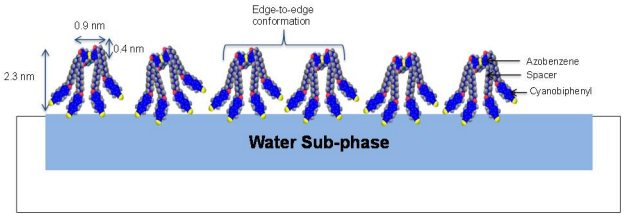

Figure 2.9: Schematic diagram of the arrangement of the molecules of compound at air-water interface.

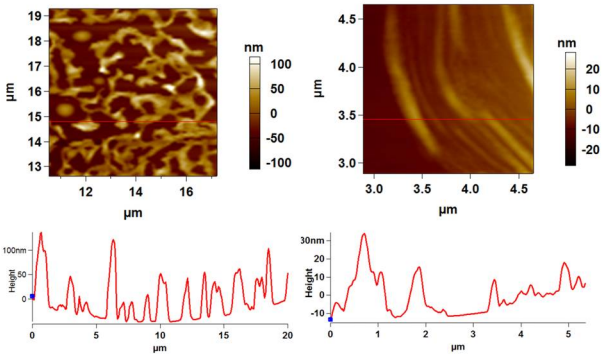

Figure 2.10: AFM topography for film of compound transferred by LB technique onto hydrophilic mica substrate at target surface pressure (π_t) of 35 mN/m showing dense fibres in (a) and aligned fibres in less dense area in (b). The respective height profiles corresponding to the lines drawn on the images are shown below.

azobenzene group extrude into the air (Figure 2.9). The limiting area per molecule calculated from the $\pi - A_m$ isotherm also indicated similar conformation of the molecule at the interface. Interestingly, in high density areas (Figure 10) the film shows network of thin fibres with varying thickness greater than 10 nm to 80 nm. The fibre like pattern on the mica substrate could be associated with the dipolar interactions and $\pi - \pi$ stacking of the cyanobiphenyl and azobenzene units. These thin fibres bundle up to form thick ones. These results when combined with the BAM images during expansion shows similar fibre network pattern with a high hysteresis) demonstrated that film at the air-solid interfaces is not a monolayer. We hypothesized that the strong dipole moment of about 3.8 Debye of the cyano groups in the biphenyl rings led to substantial dipole-dipole interactions between them which is responsible for the intercalation of the molecules showing fiber like patterns.

In the case of hydrophobic silicon substrate, coated with HMDS, two layers of the film (bilayer) get coated in one dipping cycle (i.e. deposition takes place in both downward and upward stroke). Interestingly, the AFM topography of the films showed

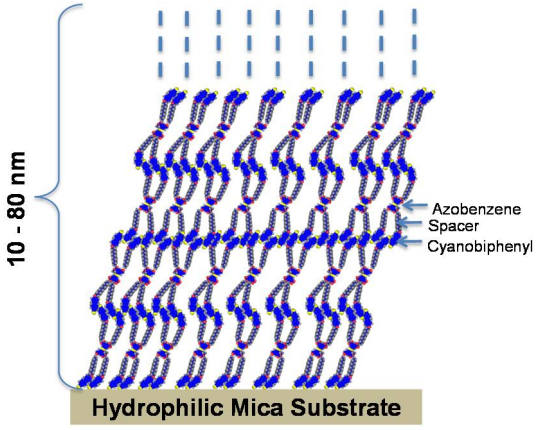

Figure 2.11: Schematic diagram of arrangement of molecules of compound at air-solid interface (mica substrate) in the high density region

the formation of nanodroplets (Figure 2.10). The height of the nanodroplets varied between 20-80 nm and did not correspond to the bilayer thickness. The droplets formations with larger heights are likely to be associated with dewetting of the film on hydrophobic silicon. Formations of such kinds of nanodroplets were observed by other groups in past. For example, Kumar et al. demonstrated that the formation of nanodroplets is due to post-transfer reorganization of the film [4]. Their study revealed that the transfer of a thin liquid film to a non-wettable solid substrates leads to formation of unstable film that eventually ruptures to the droplets through spinodal dewetting. Hashimoto and coworkers reported micrometer sized droplet (with controlled diameter and height) formation by dewetting [28]. We believe a similar mechanism is associated leading to the formation of droplets of larger height with the oligomeric mesogens synthesized in our study.

Our next study was to look the film supported on HMDS-coated silicon with respect to temperature. The study was motivated by two goals. First, we sought to characterize the film at a temperature in which compound show the mesophase. As the most intriguing properties of LC materials are exhibited at mesophase, we thought that it would be worth to look the film topography as a function of temperature. Second, by varying temperature, we sought to provide additional insight into the physicochmeical phenomena underlying the formation of nanodroplets. Figure 2.12 shows the AFM images of the LB films of TCB10 at $114\,\mathrm{deg}\,C$. This was achieved by heating the film to the isotropic temperature $126\,\mathrm{deg}\,C$ followed by cooling it to the mesophase temperature. Very interestingly, we observed well-defined aligned fibers (in the same direction) of $20-60\,\mu m$ at $114\,\mathrm{deg}\,C$ under AFM.

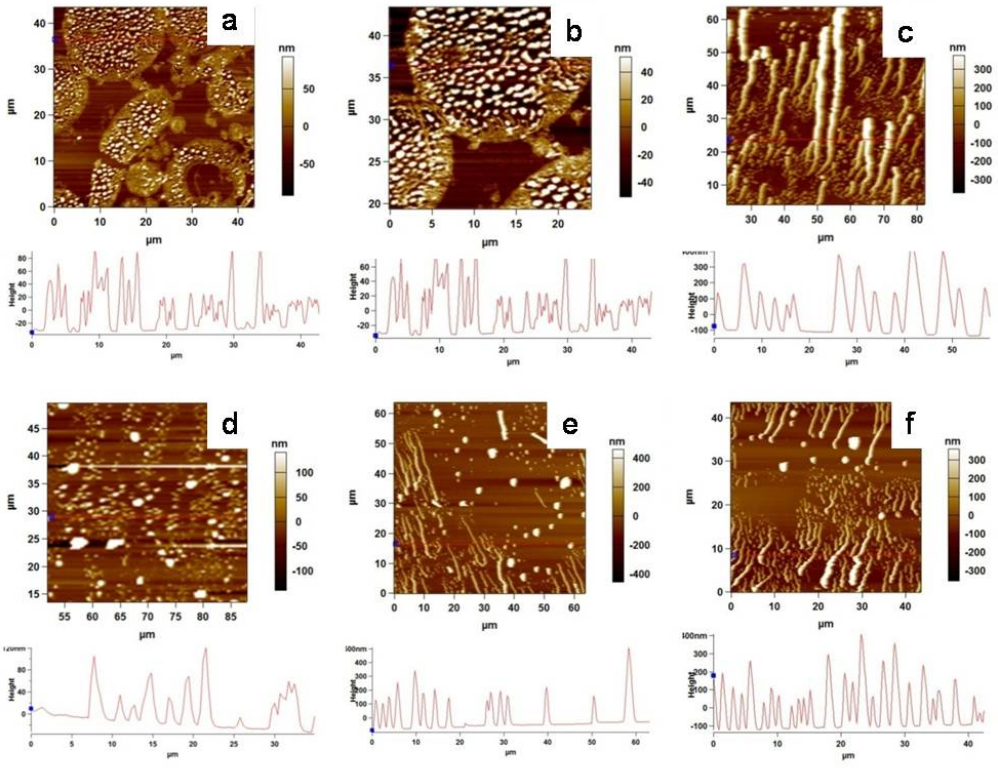

Figure 2.12: AFM topography for layer of compound transferred by LB technique onto hydrophobic HMDS coated silicon substrate at target surface pressure (π_t) of 35 mN/m. (a) LC nanodroplet formation at room temperature as shown in (b). (c) shows formation of well aligned rod like structures formed when compound is in liquid crystalline (nematic) phase at 115 deg C. (d) on cooling back to room temperature, it reverts back to nanodroplets. (e) (f) shows co-existence of rod like structures and nanoparticles at onset.

The film was cooled back to room temperature that showed again the formation of small droplets as was seen earlier prior to heating the sample in the film. This result demonstrated that LC mesophase play an important role into the formation of aligned fibres. We hypothesized that because of inherent orientational order present into the mesophase, molecules are able to self-organize themselves through supramolecular non-covalent interactions.

At room temperature, because of the crystalline nature of the molecules the thin film on hydrophobic silicon develops surface fluctuations of various wavelengths (spinodal dewetting as discussed above) and thus become unstable and ruptures in the form of droplets. Further heating to isotropic temperature and cooling back to onset temperature revealed the coexistence of both aligned fibers and the droplets. This result suggested the reversible transformation of the droplets to fibers and vice versa in the mesophase and at room temperature, respectively. We believe that the strong supramolecular non-covalent interactions in the N mesophase and in order to prevent steric hindrance from each other, these fibers align in the same direction.

2.4 Conclusions

In conclusion, the study reported in this paper is three fold. Firstly, we have synthesized eight new oligomeric mesogens consisting of an azobenzene-based core attached to which are four 4-cyanobiphenyl units via flexible alkyl spacers. Among them, compounds having octyloxy and decyloxy spacer showed monotropic N phase. Second, the novel mesogenic molecules are amphiphilic and form stable monolayer at air-water interfaces that has been characterized through surface manometry and BAM. Third, LB films transferred onto freshly cleaved hydrophilic mica substrates showed domains of height corresponding to the height of the molecule showing the formation of monomolecular film. On a hydrophobic silicon substrate, the LB transfer yield a multilayer film which could be attributed through dipolar interactions associated with the cyanobiphenyl units. The film dewets to form nanodroplets that can be attributed to spinodal dewetting. Temperature dependent AFM topography showed the reversible formation of aligned fibers in the mesophase which provides new approaches to the realization of controlling the anisotropic properties of the ordered phase.

Bibliography

[1] Mul, M. N. G.; Mann, J. A. *Langmuir* **1994**, 10, 2311.

[2] Roberts, G. *Langmuir-Blodgett Films*; Plenum Press:New York, **1990**.

[3] Kaganer, V.M.; Mohwald, H.; Dutta, P. *Rev. Mod. Phys.* **1999**, 71, 779.

[4] Kumar, B.; Prajapati, A. K.; Varia, M. C.; Suresh, K. A. *Langmuir* **2009**, 25, 839.

[5] Zhao, Y.; Chenard, Y.; Paiement, N. *Macromolecules* **2000**, 33, 1049

[6] Cui, L.; Zhao, Y. *Macromolecules* **2003**, 36, 8246.

[7] Kimizuka, N.; Kawasaki T.; Kunitake, T. *Chem. Lett.* **1994**, 23, 1399-402

[8] Anasuma, H.; Liang, X.; Yoshida, T.; Komiyama, M. *Chem. Biol. Chem.* **2001**, 2, 39

[9] Yamazawa, A.; Liang, X.; Asanuma, H.; Komiyama, M. *Angew. Chem. Int. Ed. Engl.* **2000**, 39, 2356.

[10] Serpe M. J.; Craig S. L. *Langmuir* **2007**, 23, 1626.

[11] Delphia S. R. P.; Senthil S.; Kannan P.; Vinitha G.; Ramalingam A. *J. Phys. Chem. Solids* **2007**, 68, 1812.

[12] Kumaresan S.; Kannan P. *J. Polym. Sci: Part A: Polym. Chem.* **2003**, 41, 3188.

[13] Kawatsuki N.; Unisuga S.; Neko T.; Uchida E.; Kondo M. *React. Funct. Polym.* **2009**, 69, 836.

[14] Fischer, T.; Lsker, L., Rutloh, M.; Czapla, S.; Stumpe *J. Mol. Cryst. Liq. Cryst.* **1997**, 299, 293.

[15] Del Barrio, J.; Tejedor, R. M.; Chinelatto, L. S.; Snchez, C.; Piol, M.; Oriol, L. *J. Mater. Chem.* **2009**, 19, 4922.

[16] Feng, C. L.; Zhang, Y. J.; Jin, J.; Song, Y. L.; Xie, L. Y.; Qu, G. R.; Jiang, L.; Zhu, D. B.; *Langmuir* **2001**, 17, 4593.

[17] Matsumoto, M.; Terrettaz, S.; Tachibana, H. *Adv. Colloid Interface Sci.* **2000**, 87, 147.

[18] Lui, Z.F.; Hashimoto, K.; Fujishima, A. *Nature* **1990**, 347, 658.

[19] Yamamoto, T.; Umemura, Y.; Sato, O.; Einaga, Y. *Chem. Mater.* **2004**, 16, 1195.

[20] Riul, A.; Santos, D. S.; Wohnrath, K.; Tommazo, R Di.; Carvalho, A. C. P. L. F.; Fonseca, F. J.; Oliveira, O. N.; Taylor, D. M.; Mattoso, L. H. C. *Langmuir* **2002**, 18, 239.

[21] Kumar, B.; Suresh, K. A. *Phys. Rev. E.* **2009**, 80, 021601.

[22] Velez, M.; Mukhopadhyay, S.; Muzikante, I.; Matisova, G.; Vieira, S. *Langmuir* **1997**, 13, 870.

[23] Sato, T.; Ozaki, Y.; Iriyama, K. *Langmuir* **1994**, 10, 2363.

[24] Taniike, K.; Matsumoto, T.; Sato, T.; Ozaki, Y. *J. Phys. Chem.* **1996**, 100, 15508.

[25] Hashimoto, Y.; Karthaus, O. *J. Colloid Interface Sci.* **2007**, 311, 289.

Chapter 3

Thin films of Discotic Liquid Crystals - CdSe Nanoparticles Hybrid System at Air-water and Air-solid Interfaces

3.1 Introduction

Nanomaterials are those materials which have atleast one dimension in the range of 1-100 nm.They possess unique properties, which differ from those of individual atoms or molecules and from those of bulk material.

The potential applications of nanomaterials in the fields of energy, computing, optics, catalysis, biosciences and medical sciences have been extensively discussed.[1] Like nanomaterials, LCs also possess unique properties that differ from those of either crystals or liquids. From the emergence of this strong link between nanoscience and LCs, a new term, LC Nanoscience has evolved[2,3]

Discotic Liquid crystals (DLCs), spontaneously self-assemble into nematic or columnar phases. They are generally made of a central aromatic core flanked by aliphatic chains.The strong $\pi - \pi$ interaction is mainly responsible for the formation of a columnar mesophase in the DLCs. DLCs are important functional materials which find application as one-dimensional conductors, photoconductors, light emitting diodes, optical image processing, etc.[4-7]

In the columnar phase, molecules are packed very closely, similar to molecular packing in crystalline materials. The stacking gap (intra-columnar core-core separation)

in a columnar mesophase is typically on the order of 0.35 nm, whereas the inter-columnar (between two adjacent columns) distance is typically 2-6 nm, depending on the length of lateral chains [7]. Therefore, the interactions between neighbouring molecules within the same column (intra-columnar) are much stronger than the interactions between neighbouring columns (inter columnar). Thus, the stacked molecular architecture, that is, columnar phase, can provide a facile path for the movement of generated charges via hopping from one molecule to another. Charge movement in these materials is expected to be quasi-1-D, as the conducting core of the discotic molecule is surrounded by insulating aliphatic chains [8].

Like any other organic material, DLCs are basically insulators in their virgin state; however, they can be made electrically conducting by generating charges via chemical or photochemical doping. Apart from regular dopants like bromine, iodine etc, another way to increase conductivity is incorporate metallic and semiconducting NPs into the supramolecular order of columnar phases. On the one hand, DLCs have been covalently attached to NPs. On the other hand, various functionalized NPs have been dispersed in DLCs [8].

Semiconductor inorganic NPs, commonly known as QDs, are the other 0-D NPs that have been extensively studied during the past decade because of their potential applications in the life sciences and materials science. Kumar et al. have studied the dispersion of CdSe QD in TRP [9]. They studied dispersion of two different sized CdSe quantum dots into the columnar matrix of hexabutyloxytriphenylene which indicated that insertion does not disturb the nature of the mesophase, but a minor shift in transition temperature was noticed [9]. Moreover, they found an increase of two orders of magnitude in DC conductivity [9]. Thus these CdSe QD- DLC composite systems hold a great promise in many device applications, such as photovoltaics, photoconductors, sensors etc. Dabbousi et al have studied formation of LM of monodispersed CdSe QD covered with TOPO which served as LB active species [10].

In this chapter, we have tried to study CdSe QD -DLC composites at air-water and air-solid interface. It is an ongoing work. We have used hexahexyloxytriphenylene (H6TP) as the DLC and 5 nm CdSe NPs for dispersion. Both these molecules were synthesized in RRI, Bangalore. H6TP was synthesised by Prof Sandeep and NPs were synthesised by Avinash (PhD scholar with Prof Sandeep Kumar).

3.2 Experiment

Materials and Reagents. Chemicals and solvents were all of AR quality and were used without further purification. Chloroform used for thin film studies was of HPLC grade. The compound was purified by column chromatography and recrystallization and characterized by Proton Nuclear Magnetic Resonance (^{1}H NMR), Carbon-13 Nuclear Magnetic Resonance (^{13}C NMR), Infra-red (IR), Ultraviolet-visible (UV-Vis), Raman spectroscopy and elemental analysis which indicated high purity of the material. The thermotropic liquid crystalline properties of these materials were investigated by polarizing optical microscopy, differential scanning calorimetry and small angle X-ray diffraction (XRD). NPs were purified by centrifugation and dispersion in toluene. They were characterized by transmission electron microscopy (TEM) Films of H6TP and were studied using surface manometry, BAM and AFM.

Surface Manometry

The surface manometry experiments were carried out using an APEX LB-2007 and a NIMA 611M trough. The subphase used was ultrapure deionized water obtained from Millipore Milli-Q system. The stock solution of 0.2 mg/ml concentration was prepared using chloroform (HPLC grade, Merck). Different compositions by weight of CdSe QD - H6TP were made. After spreading it on the air-water interface, the film was left for 20 min, allowing the solvent to evaporate. The $\pi - A_m$ isotherms were obtained by symmetric compression of the barriers with a constant compression rate of $10\,cm^2/min$. The surface pressure (π) was measured using the standard Wilhelmy plate technique. Film stability was also measured by measuring the variation of surface pressure (π) was measured with time keeping the area between the barriers constant.

Brewster Angle Microscopy

A Brewster angle microscope (BAM), MiniBAM (NFT, Nanotech,Germany) was employed to observe the films at the A-W interface. Instead of pressure sensor, microscope was put. Images were observed and captured during the formation of the monolayer.

Film Deposition

LB technique was employed to transfer various layers of the films onto hydrophilic substrates at target surface pressure (π_t) with a dipping speed of 1 mm/min. We have employed vertical transfer technique. For hydrophilic surfaces, freshly cleaved mica was used. For scanning transmission electron microscopy (STEM), gold grid was used for deposition by vertical LB technique. For Scanning electron microscopy(SEM) and energy dispersive x-ray spectroscopy(EDS), horizontal schaffer deposition technique was used. We used holey carbon tape as substrate which was pasted on the stub before deposition.

Atomic force Microscopy

The atomic force microscope(AFM) studies on these LB films were performed using Asylum Research MFP 3D.We used silicon tips (radius: $9 \pm 2\,nm$) with spring constant of 42 N/m and resonance frequency 300 kHz. Non-contact mode was used to obtain the topography of the film. All the images are shown without any processing.

Surface manometry, BAM and depositions were carried out at room temperature ($25 \pm 0.5 \deg C$).

3.3 Results and Discussion

Both the molecules have been previously studied to be LB active. So first, we studied the isotherms of H6TP and NPs separately. H6TP shows a typical isotherm with all the phases. The limiting area per molecule is around 1 nm^2 which corresponds to edge to edge conformation in DLC.

For CdSe QD, since we do not know the molecular mass, the measurement is made with area of the barriers. It also forms an isotherm as expected. Since both molecules can form LB, we then started study with the composites.

Then we studied different compositions for isotherm measurements. We see not much change in the isotherm, just the surface pressure for same area is higher with higher composite. This might be due to the organization change in H6TP due to insersion of NPs

The BAM images for compression shows that the molecules uniformly come together

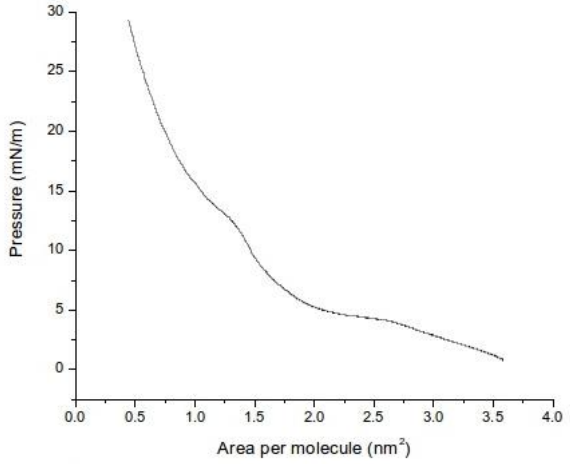

Figure 3.1: Surface Pressure (π) and Area per molecule (A_m) isotherm of pure H6TP

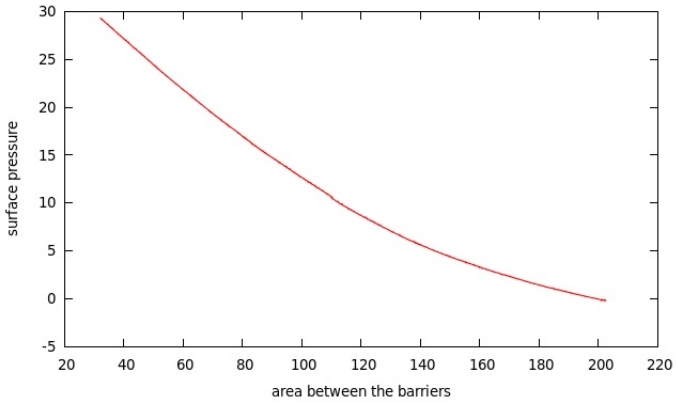

Figure 3.2: Surface Pressure (π) and Area per molecule (A_m) isotherm of CdSe NPs

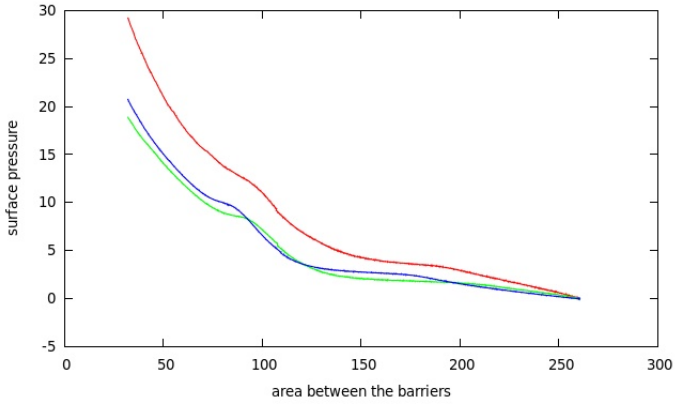

Figure 3.3: Surface Pressure (π) and Area per molecule (A_m) isotherm of increasing weight percentages. Green is for pure H6TP, blue is for 1% CdSe in H6TP and red is for 5% CdSe in H6TP

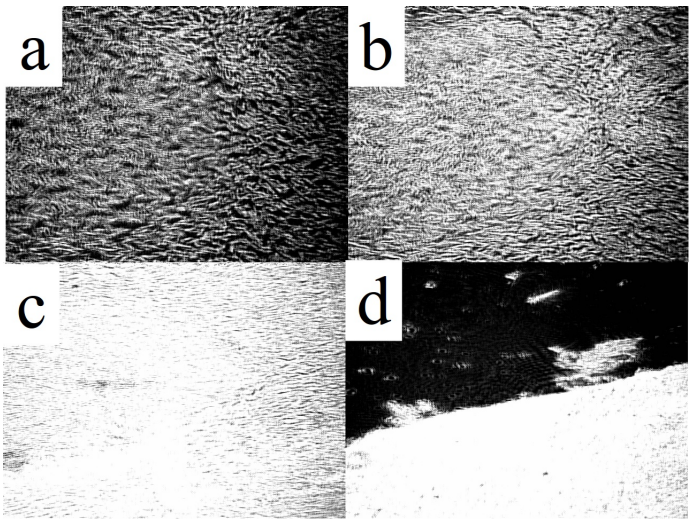

Figure 3.4: The Brewster Angle Microscopy images of compression for TCB-10 at air-water interface. The area per molecule in each case is (a) 0.2 nm^2 (liquid - condensed phase) (b) 0.1 nm^2 (monolayer) (c) 0.6 nm^2 and (d) 0.4 nm^2 (collapsed state). The scale bar in each image represents 500 μm.

and form a thin layer. We see 2D liquid and condensed phase. On further compression, when $A_m < 0.1\,nm^2$, there is uniform grey region which shows the formation of the monolayer. But on further compression, when the area per molecule is very less,there occurs a collapse for A_m of about $0.05\,nm^2$, where BAM image (figure 3.4) shows bright regions growing from the grey background.

The composite BAM is also similar to pure H6TP. We see a similar monolayer formation.

The stability of the film was checked by measuring the equilibrium surface pressure

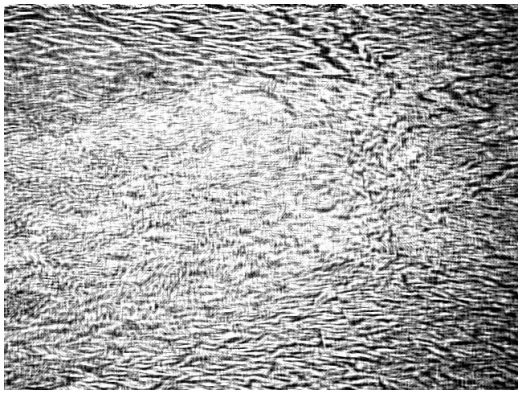

Figure 3.5: BAM image for 1% composite. The scale bar in each image represents 500 μm.

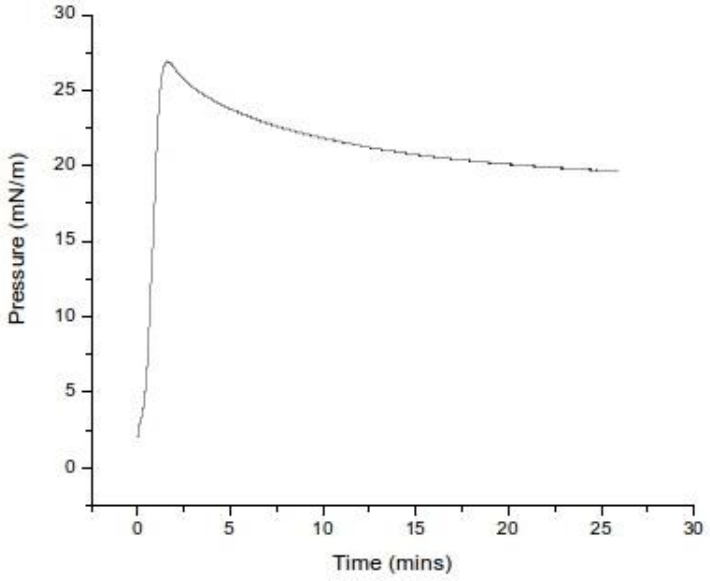

Figure 3.6: Equilibrium Surface Measurement of the composite of 1% at the surface pressure of 27 mN/m

at a constant area (figure 3.6).

we found that film was stable to carry out deposition. Then the film was deposited on hydrophilic mica by vertical dipping. In one dipping cycle, only one deposition takes place in upstroke. The resultant films were characterized by AFM.

The film was transferred onto a hydrophilic mica substrate and studied using AFM. Topography image of the LB film transferred onto a mica substrate at a surface pressure of 25 mN/m is shown in Figure

We also prepared films for STEM. But we couldn't see anything on analysis probably because the material goes inside the grid region making it difficult to observe.

To confirm insertion of NPs, we prepared films for SEM EDS. Holey Carbon itself has uniform cavities. So on deposition our film ruptures and form nanodroplets inside those cavities. Due to this it doesnt remain a uniform film. But it could still be used for EDS to confirm the insertion of NPs. But Since the quantity of CdSe QDs is very low in carbon based DLC on Carbon film, EDS was unable to detect it.

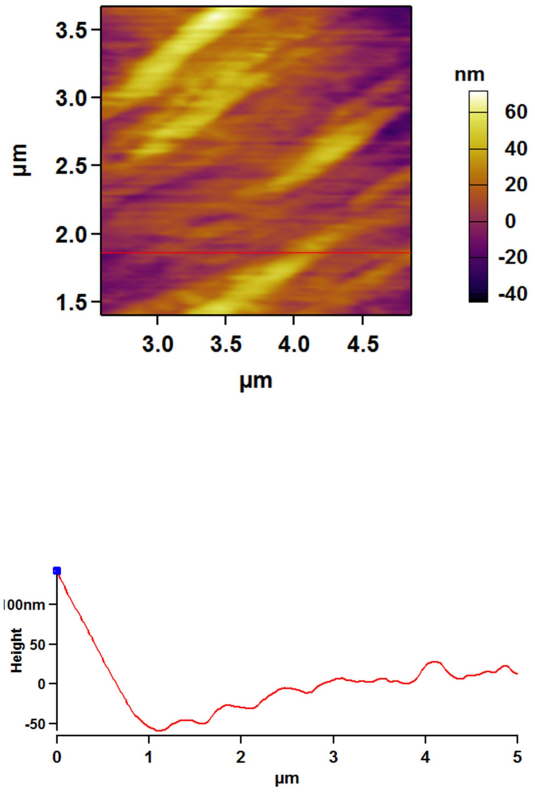

Figure 3.7: AFM topography for film of H6TP transferred by LB technique onto hydrophilic mica substrate at target surface pressure (π_t) of 25 mN/m. The respective height profile corresponding to the line drawn on the image is shown below.

3.4 Conclusions

This work is still in progress. We are in process of surely determining insertion of NPs in the H6TP. Though we do not see any phase segregation, we do not also see any any sign of incorporation of NPs in the system. After that, we would deposit the films on conducting substrate such as HOPG and determine the conductivity of pure and doped DLC. We are also trying to form bulk thick films for 2 probe and 4 probe conductivity measurements so that we can confirm presence of CdSe NPs and the change in conductivity.

Bibliography

[1] Rao, C. N. R., Muller, A. Cheetham, A. K. (eds) *The Chemistry of Nanomaterials: Synthesis, Properties and Applications* Wiley-VCH, Weinheim, **2004**.

[2] Bisoyi, H. K. Kumar, S. *Chem. Soc. Rev.* **2011** 40, 306.

[3] Garbovskiy, Y. A. Glushchenko, A. V. *Solid State Phys.* **2011** 62, 1.

[4] S. Kumar, *Chem. Soc. Rev.*, **2006**, 35, 83.

[5] S. Sergeyev, W. Pisula and Y. H. Geerts, *Chem. Soc. Rev.* **2007**, 36, 1902.

[6] J. Wu, W. Pisula and K. Mullen, *Chem. Rev.*, **2007**, 107, 718.

[7] S. Kumar, *Chemistry of Discotic Liquid Crystals: From Monomers to Polymers*, CRC Press, Boca Raton, FL, **2011**.

[8] Kumar S, *NPG Asia Materials* **2014**, 6,1.

[9] Kumar S., Sagar L., *Chem. Comm.*, **2011**, 47, 12182

[10] Dabbousi, B. O.,Rubner, M. F., Murray, C. B., Bawendi, M. G., *Chemistry of Materials*, **1994**, 6, 216.

Chapter 4

Future Work

4.1 Introduction

Apart from these, LCs find many useful applications in sensors particularly biosensors. One such biosensors that we intend to develop is for **Creatinine.**

Creatinine is the final product of creatine metabolism in mammals. The assessment of creatinine levels in human blood becomes clinically very important. It is used for the diagnosis of renal, thyroid and muscle function and is important in treatments with external dialysis.

The most commonly used assays are based on the Jaffe reaction, in which creatinine reacts with alkaline picric acid to form a colored species that absorbs at 500 nm. However, this reaction is subject to many interferences and lacks specificity. The enzymatic methods, as alternative techniques for the determination of creatinine, based on a colorimetric indication as well, offer increased accuracy. As the implementation of these methods is labor-intensive, they are mainly performed by complex automated analyzers in central laboratories.

The main development in Creatinine sensors is development in potentiometric and amperometric based devices. Amperometric biosensors have gained more importance, and since then, work has been done to make these sensors more sensitive. The focus has been on enzyme immobilization for enhanced stability.

We propose liquid crystal based biosensors for creatinine. Optical sensors using liquid-crystal materials could eliminate the need for markers or tags, as the liquid-crystal molecules act to enhance the optical appearance of signals of a biological process or structure. In observing such biosensors, label-free observations of enzymatic action

and molecular assemblies are made by detecting an optical change in the transmittance through a liquid-crystal material.
The basic principle involved it the effect of interfacial interactions. At the pure liquid-crystal/ aqueous interface, the liquid-crystal molecules tend to align planar to the surface. The introduction of contaminants (molecules for detection) induces an orientational change of the liquid-crystal material to a homeotropic alignment. During this transition, the optical appearance of the biosensor will change when viewed between crossed polarizers and this is correlated with either the identity of the contaminant and/or its concentration.

4.2 Suggested Readings

1 Madaras M. B., Popescu I. C., Ufer S., Buck R. P., *Analytica Chimica Acta* **1996** 319, 335.

2 Killard A. J., Smyth M. R., *Tibtech*, **2001**, 18, 433.

3 Jeffrey M. Brake, et al.*Science*, **2004** 302, 2094.

Appendix A

AFM topography of substrates used

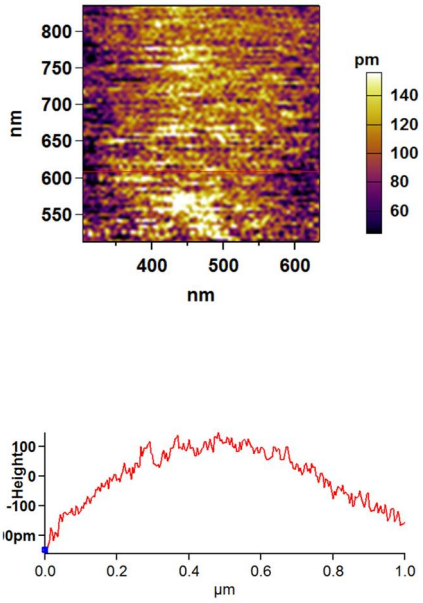

Figure A.1: AFM topography of mica substrate. The respective height profiles corresponding to the lines drawn on the images are shown below.

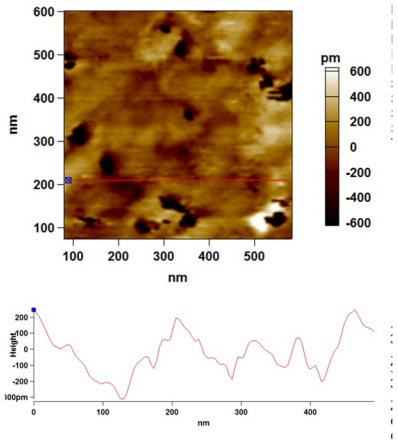

Figure A.2: AFM topography of hexamethyldisilazane coated Si substrate. The respective height profiles corresponding to the lines drawn on the images are shown below.

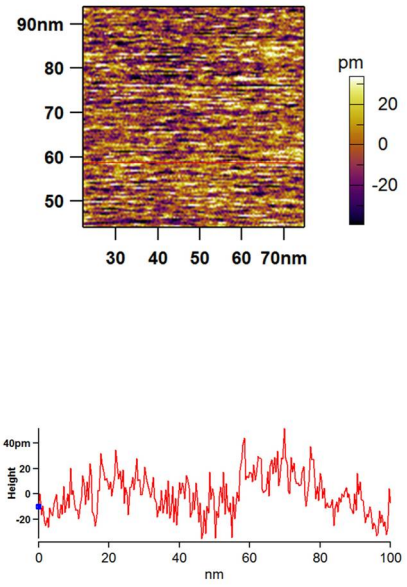

Figure A.3: AFM topography of HOPG substrate. The respective height profiles corresponding to the lines drawn on the images are shown below.